Electrical properties of compacted assembly of copper oxide nanoparticles

Anindita Bose, Soumen Basu, Sourish Banerjee, and Dipankar Chakravorty

Citation: Journal of Applied Physics **98**, 074307 (2005); doi: 10.1063/1.2084311
View online: http://dx.doi.org/10.1063/1.2084311
View Table of Contents: http://scitation.aip.org/content/aip/journal/jap/98/7?ver=pdfcov
Published by the AIP Publishing

Electrical properties of compacted assembly of copper oxide nanoparticles

Anindita Bose and Soumen Basu
Unit on Nano Science and Technology, Indian Association for the Cultivation of Science, Kolkata-700 032, India

Sourish Banerjee
Department of Physics, University of Calcutta, Kolkata-700 009, India

Dipankar Chakravorty
Unit on Nano Science and Technology, Indian Association for the Cultivation of Science, Kolkata-700 032, India

(Received 24 August 2004; accepted 30 August 2005; published online 5 October 2005)

Cu_2O nanoparticles with diameters in the range 6.0-8.6 nm were prepared by a chemical method. Both dc and ac electrical properties were measured on a compacted nanoparticle assembly. dc electrical resistivity in the temperature range 140-300 K was found to arise due to a variable range hopping conduction mechanism. The ac resistivity variation as a function of frequency (in the range 10 kHz to 3 MHz) and temperature (range 220–320 K) was explained on the basis of the power-law exponent in percolating clusters. The interfacial amorphous phase of the nanoparticle assembly appears to control the electrical behavior of the system. © *2005 American Institute of Physics*. [DOI: 10.1063/1.2084311]

INTRODUCTION

Nanomaterials research has occupied center stage in recent years.[1] Apart from understanding the basic physics[2–4] at the nanoscale, the interest has stemmed from the possibility of exploiting these materials in a wide range of applications.[5–9] A unique feature of nanomaterials is the large surface to volume ratio available in these systems. In fact the number of interfaces in a typical sample consisting of grains of 5 nm diameter has been estimated to be $10^{17}/cm^2$. In the case of silicon grain boundaries, an amorphous equilibrium phase was shown to exist.[10,11] The electrical properties of a nanocomposite consisting of a metal core-metal oxide shell nanostructure within a silica gel indicated the presence of an interfacial amorphous phase.[12] Oxide glasses are known to be formed by some building blocks like SiO_4 (in the case of silicate glasses) which have an ordered structure. The amorphousness arises because of the random interconnection of these units. One can therefore visualize the possibility of making amorphous systems starting with nanoparticles of oxides and then forming a three-dimensional compact with these. Filling the void spaces in such a system by suitable atomic and or molecular species is expected to lead to unusual glass systems. As a first step towards this objective, we have prepared nanoparticles of copper oxide and prepared pellets by cold (to avoid grain growth) compaction. Both dc and ac electrical properties have been measured. The data analysis reveals the existence of an amorphous phase controlled by the interfacial regions of the nanoparticle assembly. The details are reported in this paper.

EXPERIMENT

The nanosized Cu_2O particles were prepared by the following procedure. The first step was preparation of polyacrylamide-coated Cu_2O nanoparticles. A solution was made by dissolving a measured amount of polyacrylamide in 200 ml distilled water. The mixture was stirred by a magnetic stirrer for 6 h. Another solution was prepared by adding measured amounts of $CuSO_4$ and glucose $[CH_2OH\cdot(CHOH)_4\cdot CHO]$ to 40 ml distilled water and the mixture stirred for 1/2 h. An alkaline solution was prepared by dissolving 0.12 g NaOH pellets in 10 ml distilled water. This was slowly added to the solution comprising $CuSO_4$ and glucose, stirring until the solution acquired a deep blue color. The stirring was kept up for another hour. The *p*H of the solution was checked to be ~8.0. The alkaline $CuSO_4$ solution was slowly added to the polyacrylamide solution prepared earlier. The resultant solution was stirred for 2 h at room temperature. The solution was heated so that the temperature increased at a rate of 5 K/min. The transparent deep blue solution transformed to a pale green colloid at around 353 K. The temperature was kept constant at this point for 15 min. Cu_2O particles formed due to a partial reduction of $CuSO_4$ by glucose in the alkaline medium. The powders were collected after centrifuging for 15 min at 10 000 rpm. The powders formed were subjected to 4 h of washing in distilled water so that the polyacrylamide films were removed. The film formation was necessary in the first place to prevent the coarsening of Cu_2O particles during the reduction reaction mentioned above. On the other hand, these had to be removed so that the true electrical conduction in the interfacial region of the nanosized Cu_2O particles could be measured.

The particle sizes were measured from the micrographs taken in a JEM 200 CX transmission electron microscope. For this the polyacrylamide coated Cu_2O particles dispersed in water was taken in a test tube which was subjected to ultrasonic vibration. One drop of this mixture was placed on a carbon coated copper grid. The latter was heated at 313 K

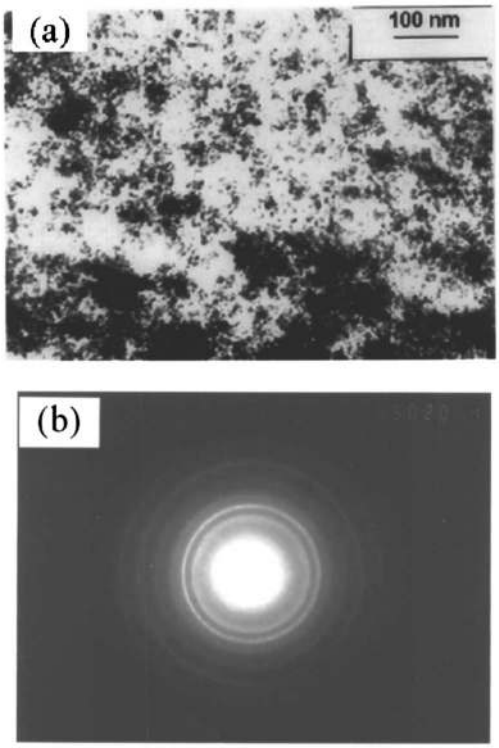

FIG. 1. (a) Transmission electron micrograph for Cu_2O specimen prepared using 0.25 g polyacrylamide, 0.625 g copper sulfate, and 0.375 g glucose. (b) Electron diffraction pattern obtained from Fig. 1(a).

for several hours and then kept in vacuum. The grid was then mounted in the specimen chamber of the transmission electron microscope.

For electrical measurements the powder was taken in a steel mould of 1 cm diameter and compacted at a pressure of 10 tons/cm^2. Silver paint electrodes (supplied by Acheson Colloiden B.V. Holland) were applied on two opposite faces of the specimen. dc electrical resistivity was measured over the temperature range 140-300 K by a Keithley 617 Electrometer. ac electrical resistivity was measured over the frequency range 10 kHz to 3 MHz and the temperature range 220-320 K using a Hewlett Packard HP 4192A impedance analyzer.

RESULTS AND DISCUSSIONS

Figure 1(a) is the transmission electron micrograph for the specimen prepared using 0.25 g polyacrylamide, 0.625 g $CuSO_4$ and 0.375 g glucose. Figure 1(b) is the electron diffraction pattern obtained from Fig. 1(a). In Table I is given a comparison between the interplanar spacings d_{hkl} obtained from the diameters of the diffraction rings in Fig. 1(b) and the standard data for Cu_2O. It is evident that the particles seen in Fig. 1(a) are comprised of Cu_2O. Figure 2 shows the histogram of Cu_2O particle sizes as obtained from Fig. 1(a). The experimental points in this figure were fitted to a log normal distribution function.[13] We have extracted the median diameter x and geometric standard deviation σ for all the specimens. These values are summarized in Table II. The latter also gives the amounts of different precursors taken for the different specimens. It can be seen that by changing the relative proportions of the starting materials the median diameter of the Cu_2O particles could be varied between 6 and 8.6 nm. It should be apparent that an increase in $CuSO_4$ concentration, as also that of the reducing agent glucose, brings about an increase in the diameter of the Cu_2O particles.

TABLE I. Comparison of d_{hkl} obtained from Fig. 1(b) with ASTM data for Cu_2O prepared from 0.25 g polyacrylamide, 0.625 g $CuSO_4$, and 0.375 g glucose.

Experiment (nm)	ASTM (nm)
0.298	0.302
0.246	0.2465
0.213	0.2135
0.174	0.1743
0.152	0.1510
0.128	0.1287

In order to delineate the conduction mechanism, we had first plotted the logarithm of dc resistivity as a function of inverse temperature. The slopes of the resultant plots gave activation energies in the range 0.20– 0.25 eV. These are much smaller than that expected for the Cu_2O nanocrystal which has a band gap of ~2.4 eV.[14] This indicates that the resistivity is not controlled by the Cu_2O nanoparticles. In Fig. 3 we have shown the variation of $\log(\rho/T)$ as a function of T^{-1} for all the specimens, where ρ is the resistivity and T is the temperature. We tried to fit the experimental data to Mott's small polaron hopping conduction model[15,16] according to which

$$\rho = \frac{kTR}{\nu_o e^2 c(1-c)} \exp(2\alpha R)\exp(W/kT), \tag{1}$$

where ν_o is the optical phonon frequency, c is the ratio of Cu^+ to the total concentration of copper ions, i.e., $[Cu^+ + Cu^{2+}]$, α^{-1} is the localization length describing the localized state at each copper ion site, R is the average intersite separation, W is the activation energy for the hopping conduction, k is the Boltzmann constant and T is the temperature. It can be seen from the figure that the data do not fit a straight line as predicted by Eq. (1)

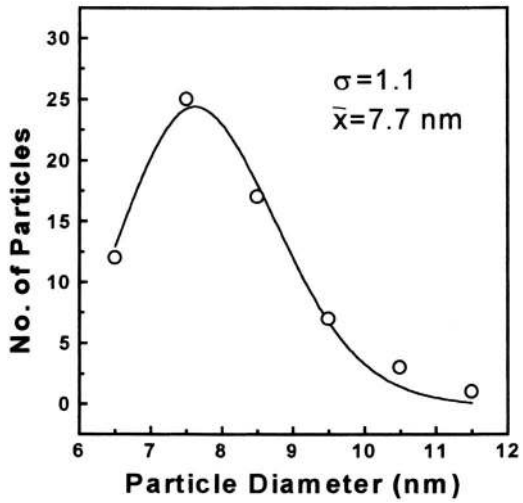

FIG. 2. Histogram of Cu_2O particles obtained from Fig. 1(a).

TABLE II. Summary of formation temperatures and extracted values of median diameter x and geometric standard deviation σ.

Specimen no.	Polyacrylamide (g)	$CuSO_4$ (g)	Glucose (g)	T_f (K)	x (nm)	σ
1	0.25	0.25	0.15	358	6.0	1.3
2	0.25	0.625	0.375	353	7.7	1.1
3	0.25	1.0	0.6	350	8.6	1.3

We have therefore used Mott's variable range hopping model[17] which gives a resistivity variation as follows:

$$\rho = \rho_0 \exp\left(\frac{T_0}{T}\right)^{1/4}, \tag{2}$$

Please check subscript zeros and ohs throughout.

$$T_0 = 2.1\left[\frac{\alpha^3}{kN(E_F)}\right], \tag{3}$$

where α^{-1} is the localization length describing the localized state at each copper ion site, $N(E_F)$ is the density of states near the Fermi level, k is the Boltzmann constant. Figure 4 shows the resistivity data plotted as a function of $T^{-1/4}$. The fitting (shown by the solid lines) with the experimental data points is satisfactory. In order to estimate the value of $N(E_F)$, we have chosen a reasonable value of α as 0.12 $Å^{-1}$ (Ref. 17) and then calculated $N(E_F)$ from the slope of the line in Fig. 4 using Eq. (3). The values of α and $N(E_F)$ are summarized in Table III. It should be noted here that in the present system some of the Cu^+ ions will get oxidized on the surface of Cu_2O particles to Cu^{2+} ions with the adsorption of O_2 molecules from the atmosphere. The hopping takes place between Cu^+ and Cu^{2+} ions. $N(E_F)$ values extracted in the present analysis are very high, being of the order of conduction or valence band states of a typical semiconductor. Cu_2O is known to be a p-type semiconductor which arises due to nonstoichiometry.[18] This discrepancy is attributed to the contribution of copper ions at the surfaces of the nanoparticles. We estimate the number of states contributing to the electrical conductivity at room temperature by multiplying $N(E_F)$ with kT_r, where T_r is equal to 300 K. This worked out to be $\sim 1.2\times 10^{21}/cm^3$ for specimen No. 1. Taking the density of Cu_2O to be 6 g/cm^3[19] we estimate a concentration of $\sim 5\times 10^{22}/cm^3$ of copper ions in Cu_2O particles. The volume of a copper oxide nanoparticle is calculated to be $\sim 1.1\times 10^{-19}$ cm^3 The number of copper ions in one such particle will be 5.6×10^3. We estimate the number of copper oxide particles in unit volume to be $\sim 8.8\times 10^{18}$. In the present system we believe only the copper ions at the interfacial region will contribute to conductivity. This number should be $\sim 10\%$ of the total copper ions present in the nanocrystals. Hence the number of localized states formed by the interfacial copper ions will be $\sim 4.9\times 10^{21}$, which is consistent with the estimated value from variable range hopping model. These are band states that are localized due to disorder at the interfaces. The experimental data of other samples are similar to the above. It appears that the number density of nanoparticles is at least two orders of magnitude lower than the number of states per unit volume taking part in the conduction process. This shows that the hopping is primarily intraparticle, i.e., takes place between states in the interfacial region of the same particle.

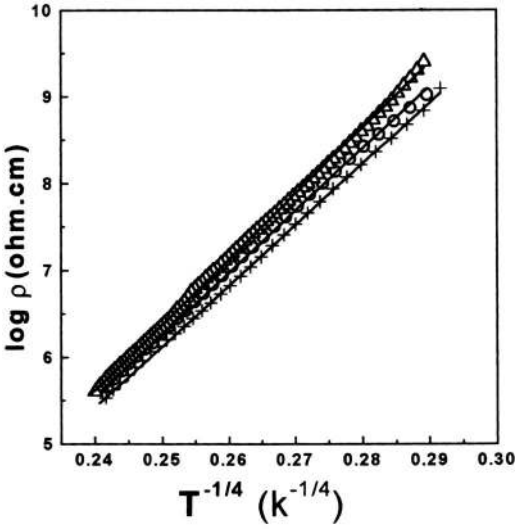

FIG. 4. Log (resistivity) as a function of $T^{-1/4}$ for different specimens. Specimen no. 1, △ ; Specimen no. 2, ○ ; + Specimen no. 3.

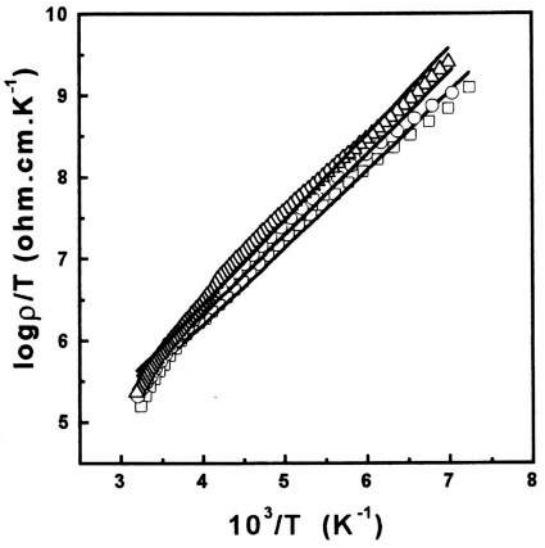

FIG. 3. Log (resistivity/temperature) as a function of inverse temperature for different specimens. Specimen no. 1, △ ; Specimen no. 2, ○ ; Specimen no. 3. □.

Figures 5(a)–5(c) show the ac conductivity variation as a function of frequency for specimens 1, 2, and 3, respectively at different temperatures. The experimental data can be represented by the equation[20]

TABLE III. Summary of parameters obtained by fitting electrical resistivity data to Mott's variable range hopping model.

Specimen no.	α ($Å^{-1}$)	$N(E_F)$ eV^{-1} cm^{-3}
1	0.12	4.7×10^{22}
2	0.12	5.8×10^{22}
3	0.12	6.9×10^{22}

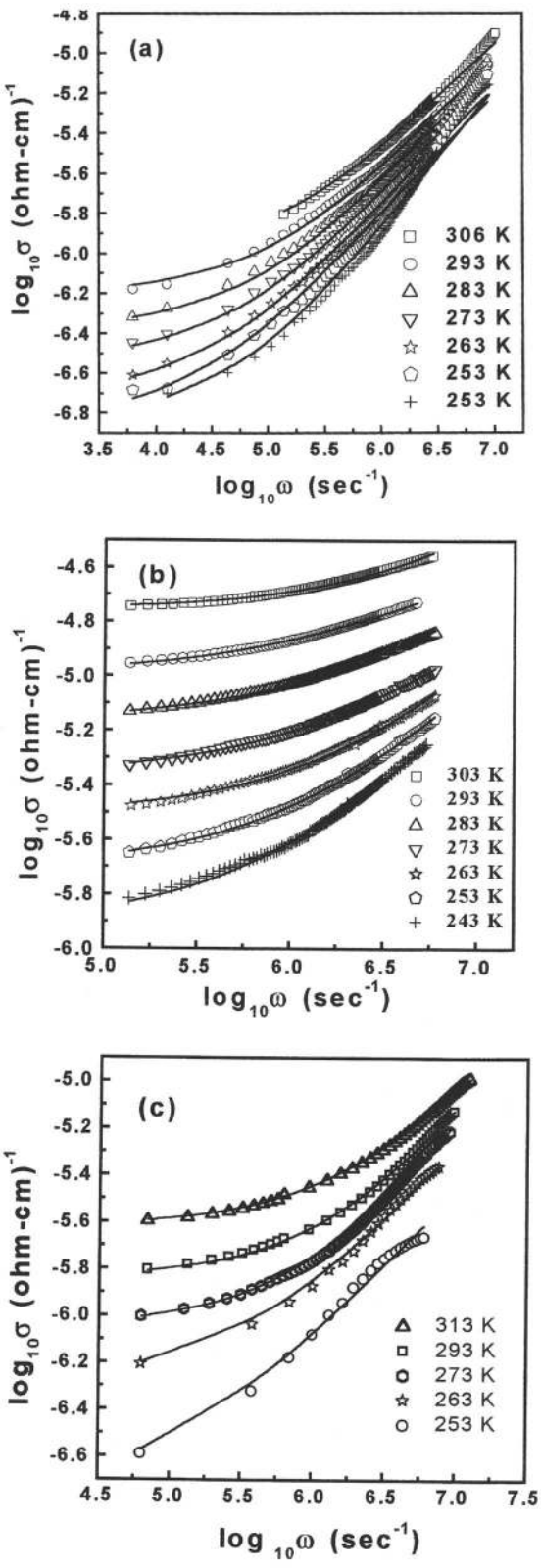

FIG. 5. Log ac conductivity as a function of frequency for different specimens (a) Specimen no. 1, (b) Specimen no. 2, (c) Specimen no. 3.

$$\sigma_{\mathrm{tot}}(\omega) = \sigma_{\mathrm{dc}} + A\omega^{s}, \tag{4}$$

where $\sigma_{\mathrm{tot}}(\omega)$ is the total ac conductivity, σ_{dc} is the dc conductivity, A is a constant, ω is the angular frequency, and s is a frequency exponent. The s values were determined from the high frequency slopes of the curves, shown in Fig. 5. These values are plotted in Fig. 6 as a function of temperature for all the specimens. It is evident that the value of s ($\sim$0.72) is independent of temperature. We explain this result by considering the theoretical model for the conduction on a distribution of clusters.[21–24] According to this model the ac conductivity $\sigma(\omega)$ is given by

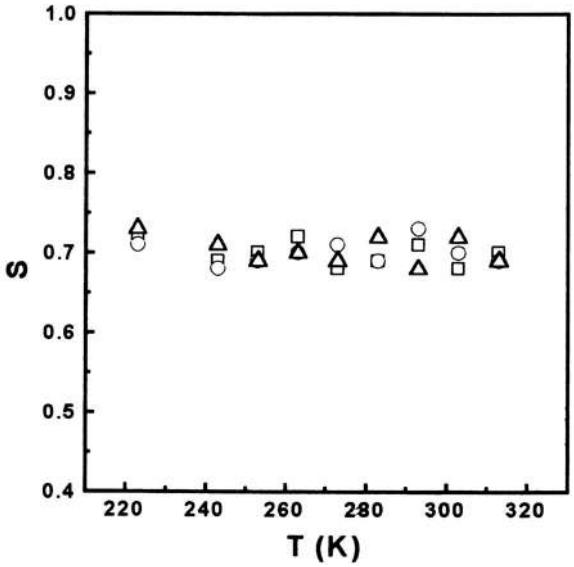

FIG. 6. Variation of s as a function of temperature for different specimens. Specimen no. 1, □ . Specimen no. 2, ○ . Specimen no. 3, △.

$$\sigma(\omega) \sim \omega^{t/(n+t)}, \tag{5}$$

where t is the power-law exponent for the dc conductivity above the percolation threshold and n is the exponent describing the divergence of the dielectric constant at the percolation threshold. For percolation clusters the theoretically calculated[25] values are $n=0.75$ and $t=1.95$. Substituting these values in the exponent as given in Eq. (5) we obtain a value of the exponent $\sigma(\omega)$ as $s=0.72$. This is in satisfactory agreement with the experimentally obtained value of s. It should be noted here that the scanning electron micrographic study of our samples showed a volume fraction of Cu_2O

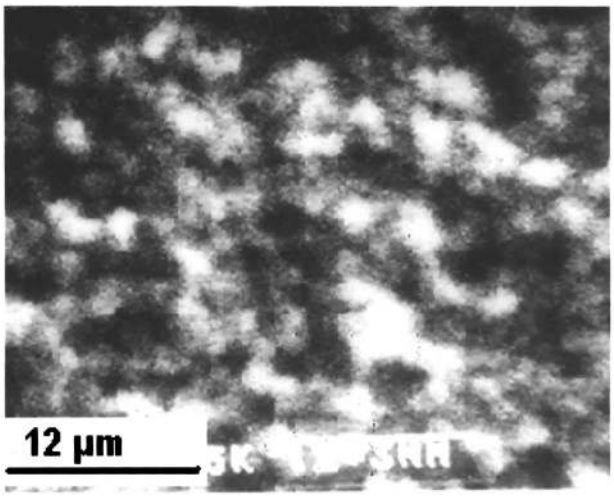

FIG. 7. Scanning electron micrograph for Specimen no. 1.

phase as 0.7—the rest consisting of void space. A typical micrograph is shown in Fig. 7. The bright regions correspond to the Cu_2O phase and the dark ones to the void phase. Evidently the Cu_2O particles have a volume fraction above the percolation threshold.

In summary, Cu_2O particles of diameter in the range 6-8.6 nm have been synthesized by a chemical method. Both dc and ac electrical properties of the cold pressed samples have been measured. dc resistivity variation as a function of temperature (140–300 K) has been explained on the basis of variable range hopping conduction between Cu^+ and Cu^{2+} ions at the interfaces of Cu_2O nanocrystals. ac resistivity variation as a function of frequency and temperature was explained on the basis of power law exponent in percolating clusters. The results indicate that the interfacial amorphous phase of the nanoparticle assembly controls the electrical properties of the system.

ACKNOWLEDGMENTS

This work has been supported by CSIR, New Delhi. Part of the research support came from a project sponsored by the Nano Science and Technology Initiative of the Department of Science and Technology, New Delhi. D. Chakravorty thanks the Indian National Science Academy, New Delhi for the award of a Senior Scientist position. S. Basu thanks CSIR, New Delhi for a Senior Research Fellowship.

[1] D. Kennedy, Science **294**, 2429 (2001).
[2] S. Morup and C. Frandsen, Phys. Rev. Lett. **92**, 217201 (2004).
[3] B. Gao, A. Komnik, R. Egger, D. C. Glattli, and A. Bachtold, Phys. Rev. Lett. **92**, 216804 (2004).
[4] I. H. Altfeder, X. Liang, T. Yamada, D. M. Chen, and V. Narayanamurti, Phys. Rev. Lett. **92**, 226404 (2004).
[5] K. I. Bolotin, F. Kuemmeth, A. N. Pasupathy, and D. C. Ralph, Appl. Phys. Lett. **84**, 3154 (2004).
[6] K. H. Kim and G. T. Kim, Appl. Phys. Lett. **85**, 5022 (2004).
[7] J. Fabian, I. Zutic, and S. Das Sarma, Appl. Phys. Lett. **84**, 85 (2004).
[8] M. Qi, E. Lidonkis, P. T. Rakich, S. G. Johnson, J. D. Joanopoulos, E. P. Ippen, and H. I. Smith, Nature (London) **429**, 538 (2004).
[9] R. Birringer, H. Gleiter, H. P. Klein, and P. Marquardt, Phys. Lett. **102A**, 365 (1984).
[10] P. Keblinski, S. R. Phillpot, D. Wolf, and H. Gleiter, Phys. Rev. Lett. **77**, 2965 (1996).
[11] P. Keblinski, D. Wolf, S. R. Phillpot, and H. Gleiter, Philos. Mag. Lett. **76**, 143 (1997).
[12] D. Das and D. Chakravorty, Appl. Phys. Lett. **76**, 1273 (2000).
[13] B. Roy and D. Chakravorty, J. Phys.: Condens. Matter **2**, 9323 (1990).
[14] S. Banerjee and D. Chakravorty, Europhys. Lett. **52**, 468 (2000).
[15] N. F. Mott, J. Non-Cryst. Solids **1**, 1 (1968).
[16] I. G. Austin and N. F. Mott, Adv. Phys. **18**, 41 (1969).
[17] N. F. Mott, Philos. Mag. **19**, 835 (1969).
[18] C. Kittel, *Introduction to Solid State Physics* (Wiley, New York, 1961), p. 354.
[19] *Handbook of Chemistry and Physics*, edited by C. D. Hodgman (Chemical Rubber Co., Cleveland, OH, 1962), p. 572.
[20] S. R. Elliott, Adv. Phys. **36**, 135 (1987).
[21] A. L. Efros and B. I. Shklovskii, Phys. Status Solidi B **76**, 475 (1976).
[22] I. Webman, J. Jortner, and M. H. Cohen, Phys. Rev. B **16**, 2593 (1977).
[23] D. Stroud and D. J. Bergman, Phys. Rev. B **25**, 2061 (1982).
[24] J. M. Luck, J. Phys. A **18**, 2061 (1985).
[25] H. J. Herrmann, B. Derrida, and J. Vannimenus, Phys. Rev. B **30**, 4080 (1984).